



City Research Online

City, University of London Institutional Repository

Citation: Xu, M., Gao, S., Guo, L., Fu, F. & Zhang, S. (2018). Study on collapse mechanism of steel frame with CFST-columns under column-removal scenario. *Journal of Constructional Steel Research*, 141, pp. 275-286. doi: 10.1016/j.jcsr.2017.11.020

This is the accepted version of the paper.

This version of the publication may differ from the final published version.

Permanent repository link: <https://openaccess.city.ac.uk/id/eprint/18616/>

Link to published version: <https://doi.org/10.1016/j.jcsr.2017.11.020>

Copyright: City Research Online aims to make research outputs of City, University of London available to a wider audience. Copyright and Moral Rights remain with the author(s) and/or copyright holders. URLs from City Research Online may be freely distributed and linked to.

Reuse: Copies of full items can be used for personal research or study, educational, or not-for-profit purposes without prior permission or charge. Provided that the authors, title and full bibliographic details are credited, a hyperlink and/or URL is given for the original metadata page and the content is not changed in any way.

City Research Online:

<http://openaccess.city.ac.uk/>

publications@city.ac.uk

Study on collapse mechanism of steel frame with CFST-columns under column-removal scenario

Man Xu¹, Shan Gao^{2*,3}, Lanhui Guo³, Feng Fu⁴, Sumei Zhang³

1. School of Civil Engineering, Northeast Forestry University, Harbin 150090, China
2. Shaanxi Key Laboratory of Safety and Durability of Concrete Structures, Xijing University, Xi'an 710123, China
3. School of Civil Engineering, Harbin Institute of Technology, Harbin 150090, China
4. Department of Civil Engineering, City University of London, London, EC1V 0HB, UK

Abstract: The quantitative design approach utilizing catenary action to prevent structure against progressive collapse has become a widely accepted design method. In this paper, a single internal column removal test was conducted for a 1/3 scale 4-bay steel frame with concrete-filled steel tubular (CFST) columns. The anti-collapse mechanism of the frame under the scenario of column loss is discussed. Both FE model and simplified analytical model are developed to investigate the behavior of steel frame with CFST columns in resisting progressive collapse. The accuracy of the two models is verified through the experimental results. The anti-collapse measures of the proposed model is sensitive to the modeling techniques used to simulate the CFST columns. A method based on the energy conservation is used to evaluate the dynamic behavior of the frame. The results show that the DAF (dynamic amplification factor) value of 2.0 which is recommended by DoD provision in linear static analysis is conservative. However, the mobilization of "catenary action" which is not considered in DoD provision would increase the DAF value as currently given in DoD.

Keywords: Progressive collapse; CFST; Composite structures; Dynamic effect

1. Introduction

Since the notorious terrorist attack of WTC in 2001, researchers and engineers have been forced to review the existing research works and standards in resisting the progressive collapse of structures. From then on, the design of structure against progressive collapse has been moving towards quantitative design approach, rather than qualitative design approach [1-2]. More and more experimental and theoretical works have been focused in this area.

In quantitative design, namely direct design method, catenary action plays a critical role to resist progressive collapse. After the failure of structural column due to abnormal loads, such as explosion, fire or vehicle strikes, the loads acting on the damaged column tend to redistribute through the beams connected to the damaged column, as shown in Fig. 1. Instead of axial force in the column, bending moment and tensile load appear in the beam and beam-column joint to resist vertical loads. The failure of beam-column joint would prevent the forming of catenary action, which would initiate local collapse, even the progressive collapse of structures.

Recently, more experimental tests are conducted and numerical and theoretical studies on progressive collapse are gradually developed in reference [3-10]. Yi *et al.* [11] tested a 3-story plane concrete frame with middle column

removal. The results indicated that the concrete frame under one damaged middle column would experience a four-phase failure process consisting of elastic phase, elastic-plastic phase, plastic phase and catenary phase. Demonceau *et al.* [12] carried out a static experiment of a composite frame under internal column removal. The relationship of moment-tensional force in the composite beams was studied. Sadek *et al.* [13] conducted a series tests of steel and concrete connections in the scenario of column removal. The failure modes of steel connections and concrete connections were studied. Li and Wang *et al.* [14] tested two full-scale steel joints subjected to column loss. The results had revealed two failure mechanisms in catenary action. Lew *et al.* [15] carried out a set of experiments on the progressive collapse performance of two concrete beam-column joints. Yi *et al.* [16] studied the anti-collapse behavior of the flat slab-column structures based on the results in Ref. [11]. Yang *et al.* [17] tested a composite frame with a middle column removal. The test results showed that more rebar should be used in the concrete slab to enhance tying force. Qian [18] proposed a simple approach which can be used to assess the vulnerability of RC structures with multiple column loss. Guo and Gao [19-20] studied the behavior of a pair of plane composite frames with different connections in the scenario of middle column loss. The results indicated the collapse process of steel frame with composite beams under single column loss was composed of six phases. “Arch action” would be mobilized in the early phase of progressive collapse.

From aforementioned studies, it can be seen that most of the research works focused on the performance of the joint atop the damaged column. As shown in Fig. 1, the joint adjacent to the removed column would sustain hogging moment and tensile force when an internal column is removed and the behavior of the adjacent joint would be different to that of the joint sitting directly above the damaged column. Meanwhile lateral stiffness of the joint which refers to the remainder of damaged structure would play a critical role in the forming of catenary action in the beams.

In this study, a 1/3 scale 4-bay steel frame with concrete-filled steel tubular (CFST) columns was tested with one internal column removed. No additional lateral restraint is applied on the structure, which is to replicate a practical boundary condition in the test. The load redistribution mechanism for steel frame with CFST columns under internal column loss will be discussed in this paper.

A simplified analytical model is proposed to simulate the response of the column-removal case. A finite element (FE) model is also developed to study the behavior of steel frame with CFST columns in resisting progressive collapse. Both models are validate through the experimental test performed in this research. In addition, dynamic amplification factor is discussed based on the simplified dynamic assessment method.

2. Experimental program

2.1. Test Specimen

In this research, a 1/3 scale 4-bay one-storey steel frame with square CFST columns was tested. The CFST columns was designed according to Chinese Code for design of Steel Structures (GB 50017-2003) and Chinese Technical Code for Concrete Filled Steel Tubular Structures (GB 50936-2014). Fig. 2 shows the detailed dimension

of the specimen. The height and the span of the scaled frame was 1.2 m and 2 m respectively. The cross section of steel beams was $H200 \times 100 \times 5.5 \times 8$ [H-overall depth \times flange width \times web thickness \times flange thickness]. Thin-wall square steel tube was used in CFST column. The width and thickness of the tube were 160mm and 5mm respectively. Outer ring plate was used in the steel-beam to CFST-column connections. The flanges of steel beam were welded to the outer ring plate whilst the web of steel beam was welded to a shear plate on the column. The shear plate was welded to the square steel tube using fillet weld. The thickness of outer ring plate and shear plate was 10mm. The middle column was removed in the experiment to simulate the scenario of column loss.

2.2. Material properties

The Chinese grade Q235 was adopted for all the structural steel members. Standard steel coupons were prepared and tested for steel members. Table 1 presents the yield stress f_y , tensile strength f_u and elastic modulus E_s of steel. The cubes of 150 \times 150 mm were tested for concrete strength whilst the prisms of 150 \times 150 \times 300 mm were tested for concrete Young's modulus. They were casted and cured in same laboratory with the specimen. The average concrete compressive strength is 33.1 MPa and elastic modulus is 2.29×10^4 MPa .

2.3. Test setup

As shown in Fig. 3(a), the CFST columns were welded to a pair of ground -beams which was screwed at the lab ground. A 500kN hydraulic jack and a load transducer were both installed atop column C as shown in Fig. 3(b). The support under column C was removed artificially. By this loading method, the anti-collapse mechanism of the frame under column removal could be observed and investigated precisely. The out-plane deformation of the specimen was restrained by a reaction frame. The load atop the column C was applied vertically with force control method until steel members began to yield. Then displacement control method was adopted in succession until the frame lost bearing capacity.

Fig. 4 shows the location of linear variable displacement transducers (LVDT). The vertical displacement of column C and horizontal displacement of column A, B, D and E were recorded by the LVDTs. Uniaxial strain gauges and strain gauges rosette were attached on the structural members as shown in Fig. 5. Only a half of the instrumentations was presented due to the symmetric configuration of the specimen.

3. Experimental observation

No evident change was observed on the specimen in elastic phase. Force control method was adopted until the vertical load reached 110 kN. At the displacement of 30 mm, slight local buckling was observed at the top flanges of the beams which is connected to column C (see Fig. 6(b)). It indicated that the joint at column C was under sagging moment. The buckling of bottom flanges was observed at the be connected to column B and column D (see Fig. 6(c)). No other evident phenomena was observed, but the buckling of flanges was aggravated. When the displacement reached 350 mm, the welding seam between beam BC and the outer ring plate of column B was fractured as shown in Fig. 6(d). Consequently the test was terminated.

Fig. 7 shows the phenomena of the frame after test. Both column B and column D were tilted towards column C under catenary action. The inward inclination also appeared at column A and column E which was not as severe as that at column B and column D (see Fig. 7(b-c)). Severe buckling appeared at both ends of steel beam BC (see Fig. 7(d-e)). The failure mode of the specimen was the fracture of welding seam between the top flange of beam BC and the outer ring plate of column B. It is worth noting that the buckling of beam flanges would not lead to the loss of bearing capacity of the specimen. On the contrary, the post-buckling strength has been developed due to catenary action.

4. Test results

4.1. Relationship of vertical load and vertical displacement

Fig. 8 shows the vertical load-vertical displacement relationship curve of column C, as well as the vertical load-horizontal displacement relationship curve of column B. This comparison was to verify various load-carrying mechanism phases of the frame. As shown in Fig. 8, the curve consists of three phases: elastic phase, plastic phase and catenary phase, except the descending phase due to unloading. The portion OA of the curve is "elastic phase" in which the vertical deformation of the frame is small, and the load-displacement relationship keeps linear. When the vertical load increases to 110 kN, the curve goes into "plastic phase" in which the relationship between the vertical load and vertical displacement is nonlinear. In this phase, the buckling of beam flanges was observed, and plastic hinges were formed at both ends of beam BC and beam CD under vertical load. Then the plastic hinge action transfers to catenary action as shown in Fig. 9. Due to the strengthening of steel material, no plastic plateau appears in the curve. The intersection point of two tangent lines on the curve in "plastic phase" is defined as plastic point [21] as shown in Fig. 8. The corresponding load resistance of plastic point is considered as plastic resistance of the specimen. Meanwhile the vertical load P can be calculated as:

$$P = 4M / L \quad (1)$$

where L stands for the length of the beam, which is 1.6 m in the test.

The theoretical value of plastic moment resistance M_p of the steel beam is 55 kN·m. Substituting M_p into Eq.(1), the calculated value of plastic resistance P_p is 137 kN which matches well with the experimental value 130 kN.

Compared with the relationship curve between vertical load and horizontal displacement at the top of column B (as shown in Fig.8), point B is verified which represents the end of "plastic phase" and the beginning of "catenary phase". Beyond point B, the horizontal displacement of column B begins to increase significantly. It means that the vertical load is resisted by "catenary action" instead of "plastic hinge action". Tying force F in Fig. 9(b) consequently increases the horizontal displacement of column B. In "catenary phase", due to the linear relationship between the vertical load and vertical displacement, the ultimate resistance P can be expressed as:

$$P = 2F \frac{\Delta}{L} \quad (2)$$

where L stands for the length of the beam, which is 1.6 m in the test.

Tying force F is supposed to be the plastic tensile resistance of steel beam. Hence the theoretical value of ultimate resistance P is 238 kN. The ultimate resistance obtained from the test is 240 kN which is 1.8 times of the

plastic resistance. It indicates that the tying force from steel beam plays a key role in catenary action. The corresponding ultimate vertical displacement is 337 mm, which is 12 times larger than the plastic displacement referring to plastic resistance. It indicates that the single-story steel frame with CFST columns which is designed and fabricated by the current Chinese specifications possesses sufficient bearing capacity and deformation capacity to prevent collapse. CFST columns provide the middle joint and beams reliable horizontal restraint to develop "catenary action".

Fig. 10 shows the relationship curves between the vertical displacement of column C and the horizontal displacement of column A and column B. Due to the symmetry arrangement of the frame, only the results of column A and column B are presented. Inwards Displacement to column C is regarded as positive. Three drop lines represent the vertical displacement of the points in Fig. 8. As shown in Fig. 10, when the vertical displacement is smaller than elastic displacement (line A), the horizontal displacement of column A and column B is almost zero which indicates that the vertical load is resisted through the bending capacity of joints. Between line A and line B, the horizontal displacements of column A and column B increase slightly with the increasing of vertical displacement. It shows that catenary action are contributing to load-carrying mechanism. Beyond the displacement at line B, the horizontal displacements at the top of columns increase remarkably until the frame failed. The discrepancy between two curves in Fig. 10 indicates that the adjacent columns to the damaged column under tying force are the primary boundary condition to the damaged structures.

4.2. Analysis of strain gauges data

Fig. 11 depicts the strain profile of the positions where plastic hinges form under different load level. The vertical line in Fig. 11(b-e) represents the yield strain of steel which is about $1334 \mu\epsilon$ in this paper. Fig. 11 shows that the strain profile of steel beam remains linear before the vertical load has arrived at 90 kN. With the increasing of vertical load, the location of neutral axis in position 1 moves upwards and the location of neutral axis in position 2 moves downwards, due to the buckling of beam flanges. When the load increases to 110 kN, the flanges of steel beam have yielded in position 1 and position 2. Due to local buckling, the strain at the top flange of steel beam in position 1 is no longer elastic and exceeds the yield strain remarkably as shown in Fig. 11(b). This discrepancy is also observed at bottom flange of steel beam in position 2. Fig. 11(d-e) depict that the joint in position 3 is under hogging moment whilst the joint in position 4 is under sagging moment.

5. Numerical analysis

5.1. Finite-element model

ABAQUS is employed to develop the finite element model replicating the aforementioned specimens. The finite element model is shown in Fig. 12. All steel components are simulated using shell element (S4R) whilst core concrete in steel tube is simulated using solid elements (C3D8R). Contact is defined between the steel tube and infilled concrete in the simulation. The friction coefficient between steel tube and infilled concrete is chosen as 0.3. Normal contact between steel tube and infilled concrete is defined as "hard contact". The mesh finess of the model has been studied to meet the analysis accuracy.

Fig. 13 shows the stress-strain relationship curves of steel and core concrete. A bi-linear relationship with stress hardening is employed as both compressive and tensile stress-strain relation of steel. The stress-strain relationships of concrete in Chinese Code for Design of Concrete Structures (GB 50010-2010) are introduced into ABAQUS. Ten percent of compressive strength and the value of 0.5 MPa are regarded as tensile strength and remaining strength in tension of concrete respectively. Meanwhile, the plastic behavior of concrete is simulated by the Concrete Damage Plasticity model in ABAQUS library.

5.2. Validation of FE model

As shown in Fig. 14, the model is validated against the test results in this study. The numerical and experimental results are in good agreement with each other. In simulation curve, no specific point is observed to distinguish plastic phase and catenary phase. As the overall performance of the structure is the major concern, the FE model is sufficiently accurate to perform the analysis. The comparison of the horizontal displacement-vertical displacement curves between the test and FE model is shown in Fig. 15. The good agreement between two curves in Fig. 15 also verifies the validity of the FE model, especially the modeling of CFST columns which directly affects the mobilization of catenary action.

Fig. 16 depicts the distribution of Von-Mises stress in the FE model. As seen, when the vertical displacement of column C reaches 110 mm which is regarded as the end of "plastic phase", both two ends of beam BC have reached yield stress 275 MPa (which are colored by red) whilst the stress level of the bottoms of column A and B is lower than yielding stress. It verifies that the load-carrying mechanism of the model is mainly through plastic hinge action. Column A and B have not been involved in load-carrying. The tensile force increases in beam BC with the increase of the vertical displacement of column C, meanwhile column A and B are mobilized as horizontal restraint for catenary action. At the vertical displacement of 330 mm, the bottoms of column A and B have reached yield strength 340 MPa under tying force.

6. Simplified analytical model

An analytical model is proposed based on experimental results. According to the affected area, the specimen under middle column loss is composed of directly affected portion (DAP) and indirectly affected portion (IAP), as shown in Fig. 17. DAP represents the damaged area of the specimen which is directly affected by the column removal. IAP represents the remainder of the specimen which acts as boundary condition of directly affected portion.

6.1. Simplified analytical model

As seen in Fig. 18, the frame can be presented by a two-span beam model with rotational restrained springs and horizontal restrained springs. The stiffness of horizontal restrained springs could be calculated by the lateral stiffness of two CFST columns as shown in Fig. 19(a):

$$K_d = K_{cl1} + K_{cl2} = 2 \cdot 12(EI)_{CFST} / L_{column}^3 \quad (3)$$

where L_{column} is the height of CFST column and $(EI)_{\text{CFST}}$ is the bending rigidity of CFST column which can be expressed as [22]:

$$(EI)_{\text{CFST}} = E_c I_c + E_s I_s \quad (4)$$

where $E_c I_c$ is the bending rigidity of core concrete and $E_s I_s$ is the bending rigidity of steel tube.

According to the configuration of beam-column connection, the rotational restraint of the simplified model should be rigid theoretically. However, the rotational stiffness of the beams and columns connected to the simplified model would affect the rotational restraint of the simplified model. Hence, a rotational restrained spring should be considered in the simplified model as shown in Fig. 19(b). The stiffness of rotational restrained springs could be calculated by the rotational stiffness of the beam and column connected to the simplified model:

$$K_r = S_c + S_b \quad (5)$$

where S_c and S_b are the rotational stiffness of the CFST column and steel beam respectively.

The remote end of steel beam and CFST column connected to the simplified model could be assumed as fixed end. Then the rotational stiffness of the beam and column can be expressed as:

$$S_b = \frac{4EI_b}{L_b} \quad (6)$$

$$S_c = \frac{4(EI)_{\text{CFST}}}{L_{\text{column}}} \quad (7)$$

The simplified model with restrained springs could be used to describe the behavior of the frame under column loss.

6.2. Validation of simplified analytical model

Although the FE model could present the collapse behavior of steel frame with CFST columns, the simulation of CFST columns have higher computational cost and bring difficulty in the convergence. The simplified model proposed in this study could be used to analyze the collapse performance of steel frame with CFST columns in practice. Based on the simplified model as shown in Fig. 18, the properties of springs are incorporated into ABAQUS model. Beam elements (B31) are used to simulate steel beam and CFST column. The profile section of middle CFST column is determined by the unified theory of concrete filled steel tube in Ref. [22].

Fig. 20 shows that the result based on simplified model prediction is in a close agreement with experimental result. The accuracy of the proposed simplified model has also been confirmed. Due to the simplification of CFST columns, the crack of core concrete in steel tube could not be considered in the simulation. Hence the difference between these two curves becomes obvious with increasing of vertical displacement. More studies on the modeling of CFST columns considering the crack of core concrete should be done in the future.

7. Discussion of DAF based on a simplified approach by Izzuddin et al. [5]

It is worth noting that the aforementioned studies are all on the basis of nonlinear static responses. This assumption is only valid in the scenario of slow column removal. However, Nonlinear dynamic analysis is more applicable for a sudden-column-removal scenario when the structures exhibit nonlinear dynamic responses. And it

is time-consuming and complicated. A simplified method to evaluate the dynamic response of structures was proposed by Izzuddin et al. [5]. As shown in Fig. 21, based on a nonlinear static response, the maximum dynamic response can be determined from the equivalence between internal energy and external work, which can be expressed by Eq. (8):

$$P_{0,n} = \frac{1}{u_{d,n}} \int_0^{u_{d,n}} P du_s \quad (8)$$

According to Eq. (8), the level of suddenly load $P_{0,n}$ causing the maximum dynamic displacement ($u_{d,n}$) equals to the mean static resistance for displacement up to $u_{d,n}$ [5].

By using this simplified dynamic assessment, the dynamic resistance of steel frame with CFST columns under a sudden column-loss is obtained. Fig. 22 shows the dynamic response of steel frame with CFST columns. It indicates that the dynamic resistance is smaller than static resistance at any displacement. In addition, according to the static response and dynamic response, the ratio of static load to dynamic load is defined as dynamic amplification factor (DAF). Fig. 23 shows the DAF calculated by the results in this study and the values calculated by DoD [1]. The DAF of current study remains almost 2.0 when the displacement is small. It indicates that the DAF value of 2.0 which is recommended to use in linear static analysis is reasonable.

With the increasing of vertical displacement, the DAF decreases remarkably. Before the vertical displacement reaches 110 mm, the trend of the curves between current study and DoD matches well, even some distinction still exists. However, when the vertical displacement is larger than 110 mm, the DAF in current study begins to increase, whilst the DAF in DoD continues to decrease. This difference could be explained by the fact that catenary action could enhance static resistance enormously which is not considered in DoD provisions. As shown in Fig. 8, the point associated with the vertical displacement of 110 mm is regarded as the beginning of "catenary phase". The mobilization of "catenary action" would increase the DAF value. Even though the catenary action is not considered, the DAF recommended in DoD provision is still convinced and could be easily used in practical project. More study in the future should be focused on the catenary action in dynamic analysis.

8. Conclusions

A steel frame with CFST columns was tested in this paper. The failure mechanism of the specimen with internal column loss is investigated in details. A FE model and a simplified analytical model are also developed. The dynamic behavior of the frame is also studied by using a simplified dynamic assessment. The following conclusions are drawn:

1. The anti-collapse mechanism of the steel frame with CFST columns involves three phases: elastic phase, plastic phase and catenary phase. The single-story steel frame with CFST columns which is designed and fabricated by the current Chinese specifications possesses sufficient load-bearing strength and deformation capacity to prevent collapse

2. Both the FE model and the simplified model could well present the behavior of steel frame with CFST columns under internal column loss. Two different simulation methods on CFST columns are used in two models. The progressive collapse resistance of the model is sensitive to the simplification of CFST columns. More studies should be done on the simplification of CFST columns considering the crack of core concrete.

3. For this particular type of structures, the DAF value of 2.0 which is recommended to use in linear static analysis is reasonable. The mobilization of "catenary action" would increase the DAF value as presently given in DoD. Even though the catenary action is not considered, the DAF recommended in DoD provisions is still convincing.

Acknowledgements

The project is supported by National Key R&D Program of China (NO. 2016YFC0701201), National Natural Science Foundation of China (NO. 50878066 and NO. 51408106) and Scientific Research Program Funded by Shaanxi Provincial Education Department (Program No. 17JK1154) which are gratefully acknowledged.

References

- [1] Department of Defense (DoD). Unified facilities criteria (UFC): design of structures to resist progressive collapse. Washington (DC). 2013.
- [2] United States General Services Administration (GSA). Progressive collapse analysis and design guidelines for new federal office buildings and major modernization projects. Washington (DC). 2003.
- [3] Buscemi N., Marjanishvili S. SDOF model for progressive collapse analysis. Proceedings of the 2005 Structures Congress. ASCE. 2005.
- [4] Khandelwal K., El-Tawil S. Collapse behavior of steel special moment resisting frame connections. Journal of structural engineering. 2007, 133(5):646-655.
- [5] Izzuddin B.A., Vlassis A.G., Elghazouli A.Y., Nethercot D.A. Progressive collapse of multi-storey buildings due to sudden column loss-Part 1: Simplified assessment framework. Engineering Structures, 2008,30(5): 1308-1318.
- [6] Xu G.Q., Ellingwood B.R. An energy-based partial pushdown analysis procedure for assessment of disproportionate collapse potential. Journal of Constructional Steel Research, 67(2011):547-555.
- [7] Li Y., Lu X.Z., Guan H., Ye L.P. An improved tie force method for progressive collapse resistance design of reinforced concrete frame structures. Engineering Structures, 33(2011):2931-2942.
- [8] Iribarren S.B., Berke P., Bouillard Ph., Vantomme J., Massart T.J.. Investigation of the influence of design and material parameters in the progressive collapse analysis of RC structures. Engineering Structures, 33(2011):2805-2820.
- [9] Gerasimidis S., Sideri J. A new partial-distributed damage method for progressive collapse analysis of steel frames. Journal of Constructional Steel Research, 119(2016):233-245.
- [10] Yu X.H., Lu D.G., Qian K., Li B. Uncertainty and Sensitivity Analysis of Reinforced Concrete Frame Structures Subjected to Column Loss. Journal of Performance of Constructed Facilities, 2016, 04016069:1-14.
- [11] Yi W.J., He Q.F., Xiao Y. Collapse performance of RC frame structure. Journal of Building Structures, 2007, 28(5):104-117. (in Chinese)
- [12] Démonceau J.F., Jaspart J.P. Experimental test simulating a column loss in a composite frame. Advanced Steel Construction, 6(2010):891-913.
- [13] Sadek F., Main J.A., Lew H.S., Bao Y.H. Testing and analysis of steel and concrete beam-column assemblies under a column removal scenario. Journal of Structural Engineering, 9(2011):881-892.
- [14] Li L., Wang W., Chen Y.Y., Lu Y. Experimental investigation of beam-to-tubular column moment connections under column removal scenario. Journal of Constructional Steel Research, 2013, 88(5): 244-255.

- [15] Lew H.S., Bao Y., Pujol S., et al. Experimental study of reinforced concrete assemblies under column removal scenario. *ACI Structural Journal*, 2014, 111(4): 881-892.
- [16] Yi W.J., Zhang F.Z., Kunnath S.K. Progressive collapse performance of RC flat plate frame structures. *Journal of Structural Engineering*. 2014, 140(9): 758-782.
- [17] Yang B., Tan K.H., Xiong G., Nie S.D. Experimental study about composite frames under an internal column-removal scenario. *Journal of Constructional Steel Research*, 121(2016): 341-351.
- [18] Qian K., Li B., Zhang Z.W. Influence of multicolumn removal on the behavior of RC floors. *Journal of Structural Engineering*. 2016, 142(5): 04016006.
- [19] Guo L.H., Gao S., Fu F., Wang Y.Y. Experimental study and numerical analysis of progressive collapse resistance of rigid composite frames. *Journal of Constructional Steel Research*, 2013, 89: 236-151.
- [20] Guo L.H., Gao S., Fu F. Structural Performance of semi-rigid composite frame under column loss. *Engineering Structures*. 2015, 95:112-126.
- [21] Bao W. Performance of partial-depth end-plates beam-to-column composite joints of steel frames under hogging moment. China: Harbin Institute of Technology, 2006. (in Chinese)
- [22] Zhong Shantong. Unified theory of concrete filled steel tube: research and application. Beijing: Tsinghua University Press, 2006. (in Chinese)

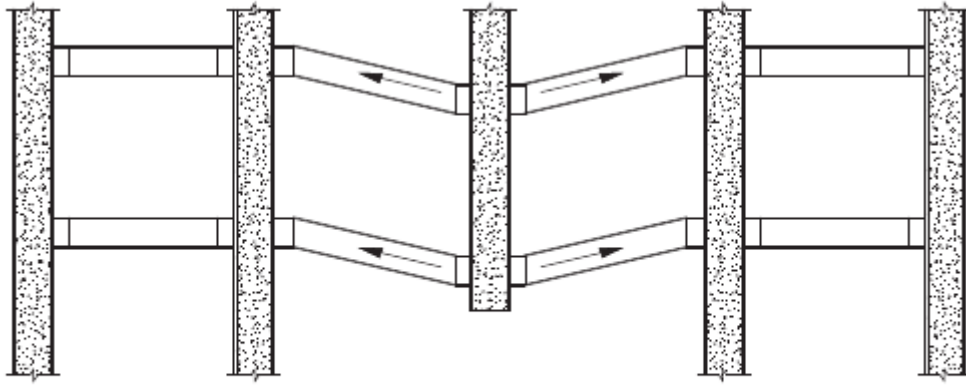
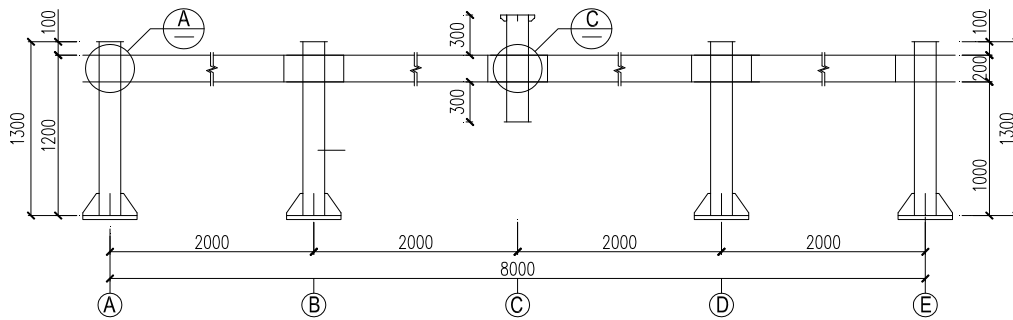
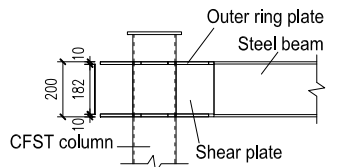


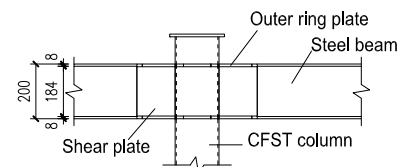
Fig 1. Catenary action.



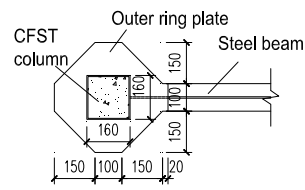
(a) Detail dimension of frame (mm)



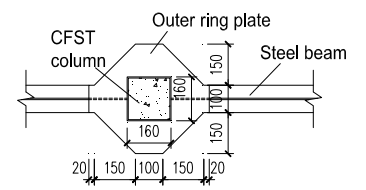
(b) Joint A



(c) Joint C (Joint B)



(A)

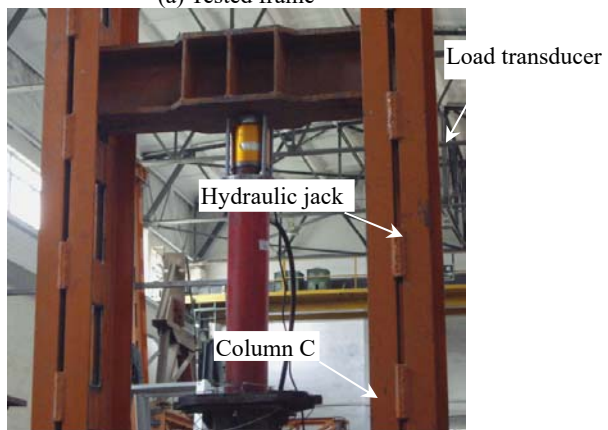


(C)

Fig. 2 Details and layout of frame



(a) Tested frame



(b) Loading equipment
Fig. 3 Experimental setup

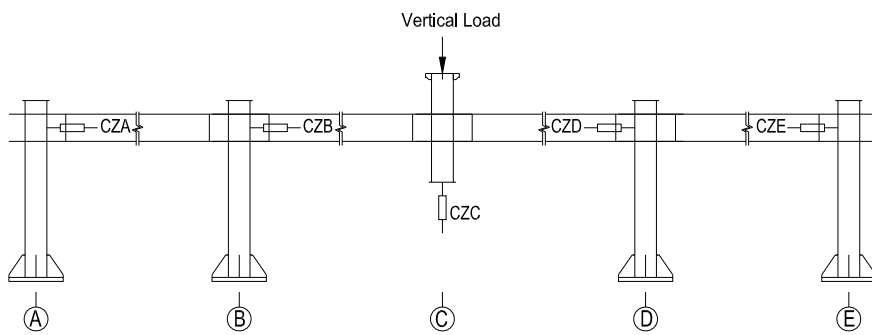


Fig. 4 Distribution of LVDTs

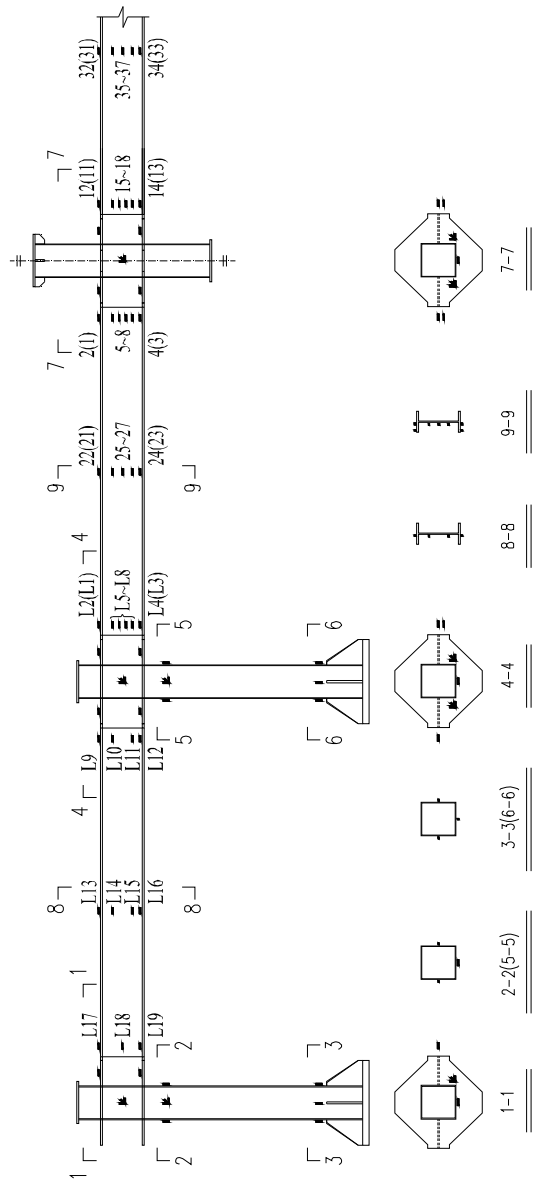


Fig. 5 Distribution of strain gauges and rosettes



(a) Positions of observation



(b) Buckling of beam in joint C



(c) Buckling of beam in joint B



(d) Fracture of weld seam in top flange

Fig. 6 Phenomena during testing



(a) Overall experimental phenomenon



(b) Inclination of column A



(c) Inclination of column B



(d) Buckling of beam in joint B



(e) Buckling of beam in joint C

Fig. 7 Phenomena after experiment

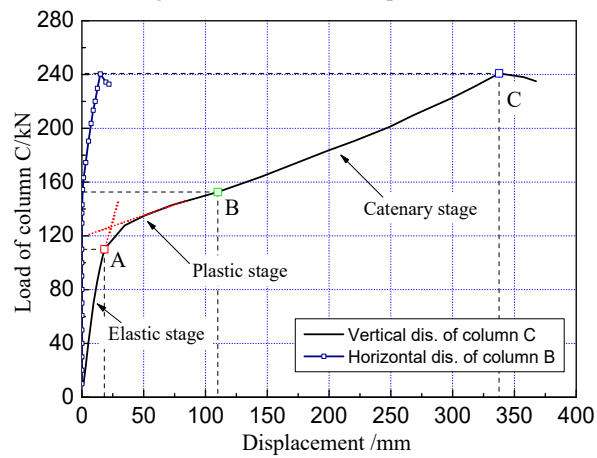
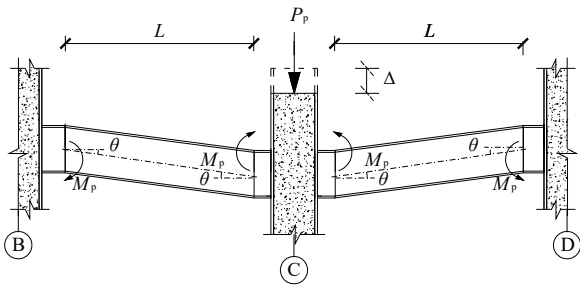
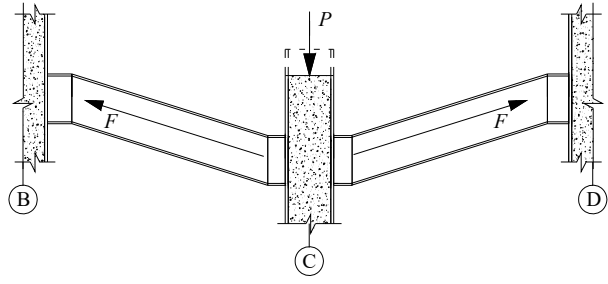


Fig.8 Vertical load-displacement of middle column curves



(a) Plastic hinge action



(b) Catenary action

Fig. 9 Load-carrying mechanism

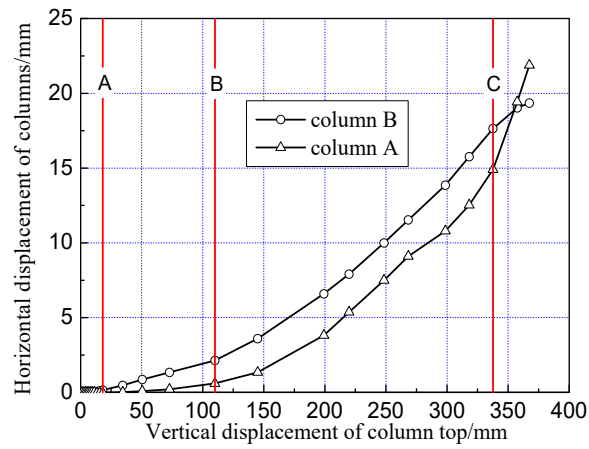
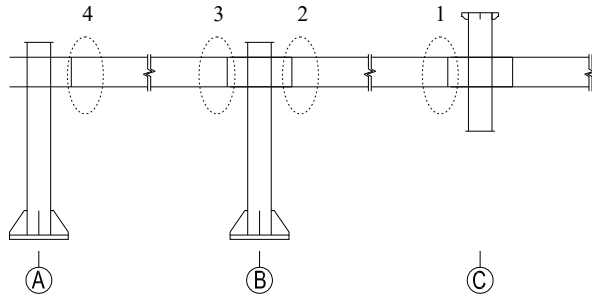
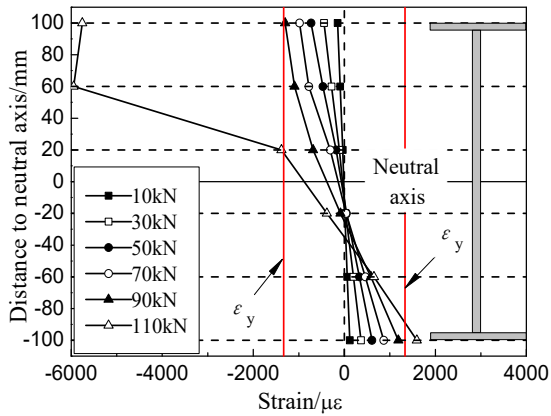


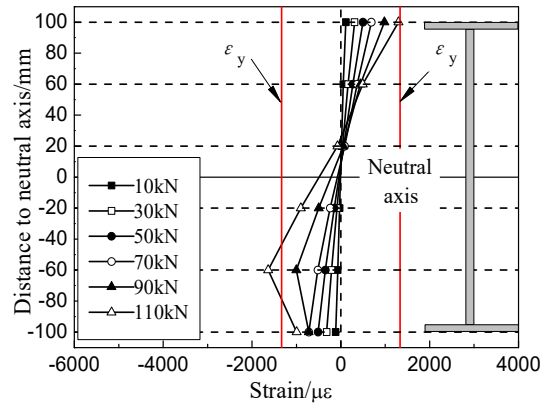
Fig. 10 Horizontal displacement-vertical displacement of column top curves



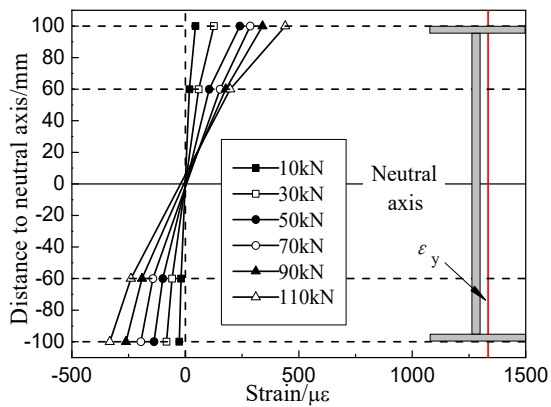
(a) Positions of strain measurement



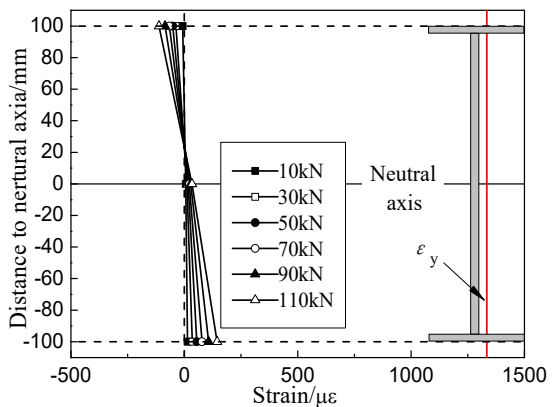
(b) Strain along the height of steel beam at position 1



(c) Strain along the height of steel beam at position 2



(d) Strain along the height of steel beam at position 3



(e) Strain along the height of steel beam at position 4

Fig. 11 Strain of steel and reinforcement

Fig.14 Simplification of restraint condition

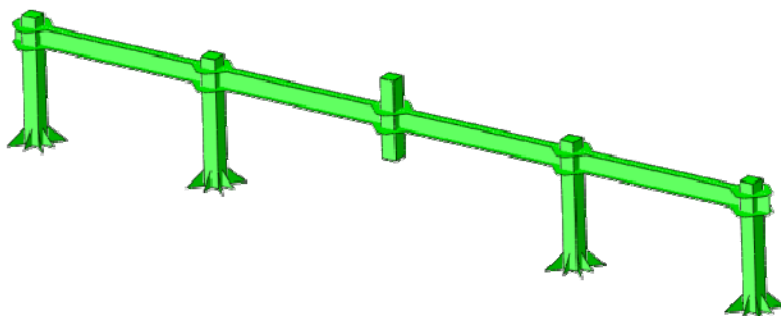
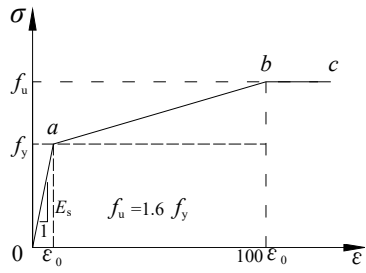
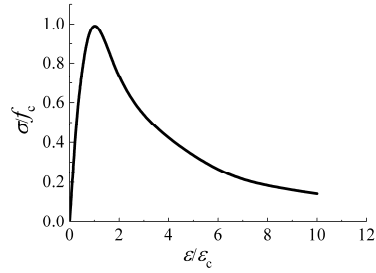


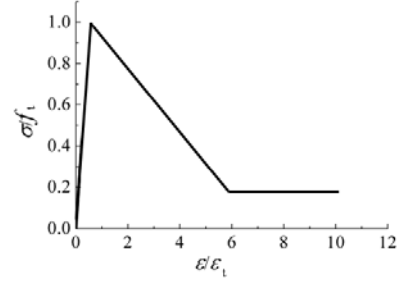
Fig. 12 The FE model



(a) Steel



(b) Concrete in compressive



(c) Concrete in tension

Fig. 13 Stress-strain relationship

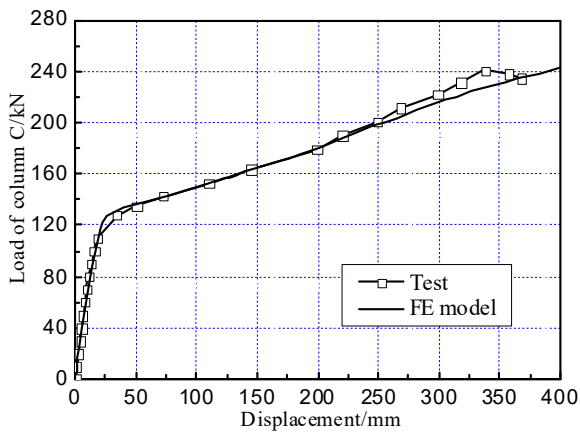


Fig. 14 Comparison of vertical load-vertical dis. of column C

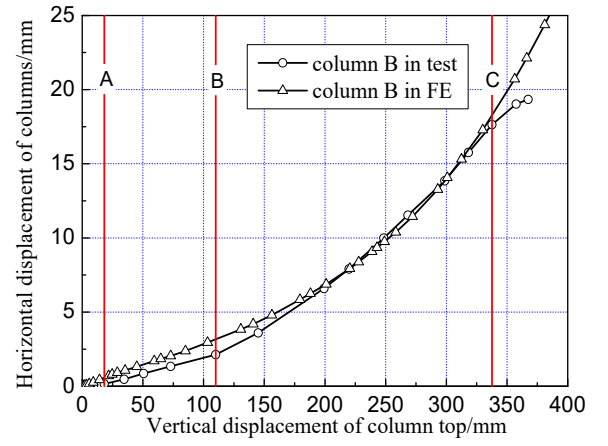


Fig. 15 Comparison of horizontal dis.-vertical dis. of column B

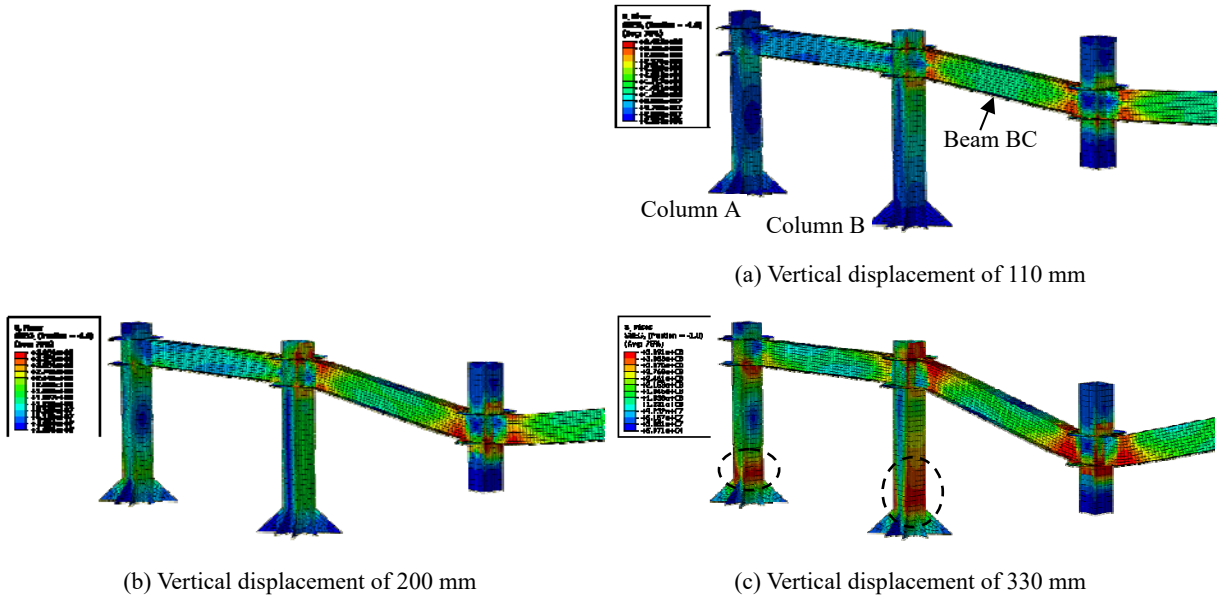


Fig. 16 Mises stress of FE model

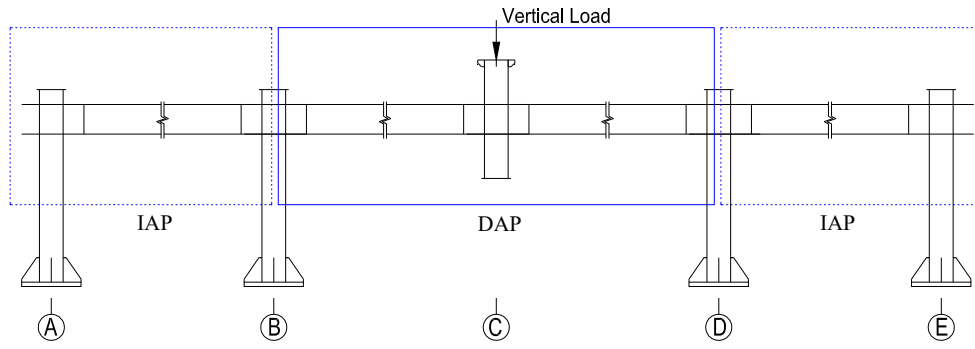


Fig. 17 Definition of DAP and IAP

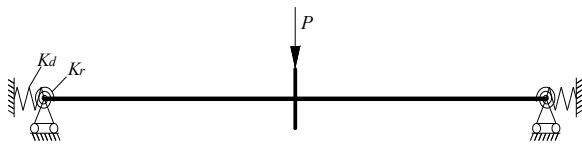
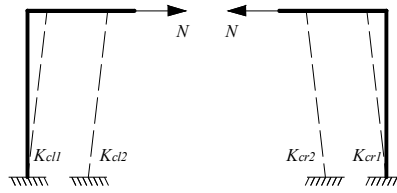
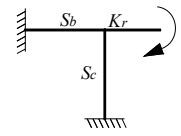


Fig. 18 Simplified mechanics model



(a) horizontal restrained spring



(b) rotational restrained spring

Fig.19 Simplification of restraint condition

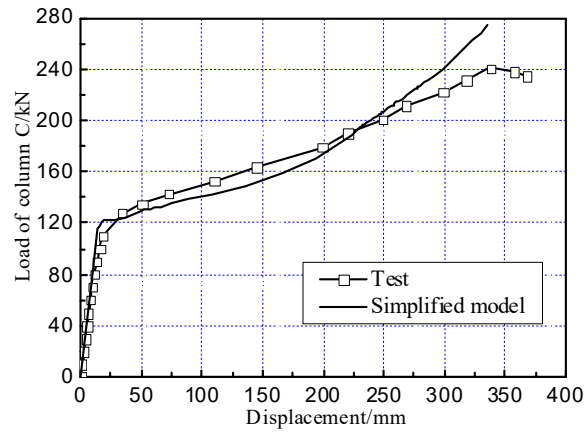


Fig. 20 Comparison of vertical load-vertical dis. of column C

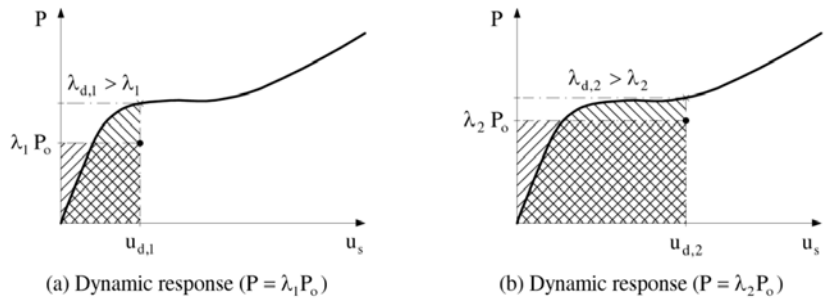


Fig. 21 Simplified dynamic assessment [5]

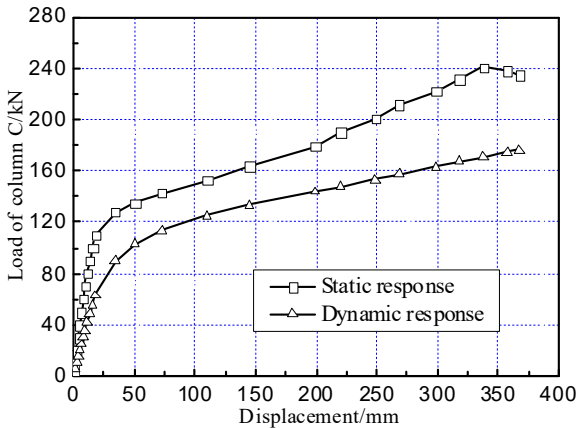


Fig. 22 Comparison of static response and dynamic response

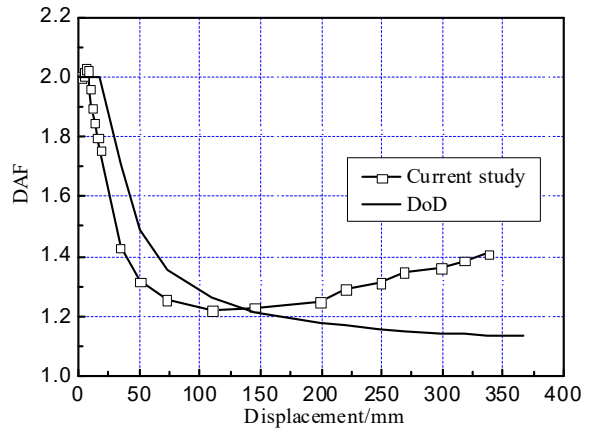


Fig. 23 Dynamic amplification factor

Table 1 Mechanical properties of steel

Se.		f_y (Mpa)	f_u (Mpa)	E_s (10^5 Mpa)
Beam	Flange	269	401	1.96
	Web	275	411	2.09
	Tube wall	342	402	1.82
	Ring plate/ Shear plate	298	388	1.91